



N6715252

ON ROLL LOCK-IN IN UNGUIDED ROCKETS

UNIVERSITY OF NOTRE DAME

AUG 1966

ON ROLL LOCK-IN IN UNGUIDED ROCKETS

John D. Nicolaides
Stephen C. Stumpfl

University of Notre Dame

CONFERENCE ON
UNGUIDED ROCKET BALLISTICS
1966
UNIVERSITY OF TEXAS AT EL PASO
August, 1966

Details of illustrations in
this document may be better
studied on microfiche

Prepared for the
NATIONAL AERONAUTICS AND SPACE ADMINISTRATION
Washington, D. C.

under Contract NSR-15-004-016

ON ROLL LOCK-IN IN UNGUIDED ROCKETS

John D. Nicolaides*
Stephen C. Stumpfl**

University of Notre Dame

ABSTRACT

The free rolling motion of three sounding rocket type configurations is studied in a wind tunnel at supersonic speeds.

It is found that the models fail to roll when the angle of attack exceeds some critical value.

The roll oscillations of the models about the roll trim angle are studied both theoretically and experimentally. The Roll Lock-In Theory is "fitted" to this experimental data and found to accurately represent the oscillations in supersonic Roll Lock-In. Also, accurate values for the (1) Roll Trim Angle, (2) the Induced Roll Moment Stability Coefficient, and (3) the Roll Damping Moment Stability Coefficient are obtained.

Abnormalities in the observed free rolling motions are also discussed.

Roll Lock-In is found to be due to the fins alone and new configurational studies are suggested.

*Chairman and Professor, Aero-Space Engineering

** Research Assistant, Aero-Space Engineering

INTRODUCTION

Inaccuracy and dispersion in sounding rockets arise from two basic causes, first, conditions in the neighborhood of the launcher and wind, and, second, dynamic instabilities arising during free flight.

This paper is concerned with free flight dynamic instabilities which, in general, fall into three categories, (1) Arrow Instability, (2) Catastrophic Yaw, and (3) Magnus Instability^{1,2,3}. While the latter two instabilities have often been observed in standard ordnance (i.e., bombs, finned projectiles, mortars, etc.), they have not been observed in sounding rockets, until recently, and even now, they are far from fully appreciated. Only three papers^{4,5,6} exist which show the importance of Magnus Instability in sounding rockets.

This particular study relates to the possibility of Catastrophic Yaw in sounding rockets. More specifically, it is concerned with the necessary condition for Catastrophic Yaw which is Roll Lock-In.

Roll Lock-In and Catastrophic Yaw have been observed in bombs at subsonic speeds. The occasional abnormal flight performance of the Aerobee Rocket suggested that perhaps Catastrophic Yaw and Roll Lock-In might occur at supersonic speeds. Thus, a special wind tunnel program was devised to determine whether Roll Lock-In could exist at supersonic speeds.

Roll Lock-In was experimentally and theoretically studied at supersonic speeds on three configurations, (1) the Basic Finner, (2) the Aerobee Rocket, and (3) the Aerobee Rocket Fins, by themselves.

EXPERIMENTAL TECHNIQUE

Models of the three configurations were mounted on ball - bearings on an aft sting. The models were placed in a supersonic stream at various angles of attack and their rolling motion was observed. Specifically, the roll angle was accurately measured as a function of time, $\gamma(t)$.

The Basic Finner model, Fig. 1, was tested at the Naval Ordnance Laboratory* at a Mach number of 3.5. The roll angle of the model was obtained from moving pictures taken with a high speed camera viewing from the side.

The Aerobee Rocket model, Fig. 2, and the Aerobee Fins model, Fig. 3, were tested at the University of Notre Dame at a Mach number of 1.41. The roll angle of the models was obtained from moving pictures taken with a Fastax camera viewing directly down the roll axis of the model, Fig. 4.

The rolling motions obtained in this manner were quite interesting and are illustrated in Figs. 5-8. It is clear that Roll Lock-In existed for all configurations. The data also shows various roll dynamic instabilities including Roll Break-Out and Roll Speed-Up. The purpose of this paper is to analyze and discuss these rolling motions.

*The University of Notre Dame is indebted to Mr. Frank Regan of the Naval Ordnance Laboratory for these excellent tests.

ROLL LOCK-IN THEORY

In the free flight case, Roll Lock-In exists when the rolling velocity of the missile is forced, by the Induced Roll Moment, to remain the same as the frequency of the wobbling motion. This condition is most often seen when the missile rolling velocity equals the nutation rate ($p_{ss} = \omega_n$). However, it can also exist for any rolling velocity when the wobbling motion is composed of only the rolling trim (K_3). In both of these cases the roll angle of the missile with respect to the plane of the complex angle of attack, γ , is constant.

In the wind tunnel case, Roll Lock-In exists when the model will not roll at angles of attack greater than zero but will roll when the angle of attack is zero. Then, again, γ is a constant.

In the following paragraphs the basic mathematics of Roll Lock-In is summarized.

The basic linear roll moment equation may be written as:

$$L(\delta_A) + L(p) = I_x \dot{p} \quad (1)$$

where $L(\delta_A)$ is the roll moment due to fin cant, $L(p)$ is the roll damping moment, I_x is the axial moment of inertia and \dot{p} is the rate of change of the rolling velocity.

From the observed dependence of Roll Lock-In on both α and γ , it is known that a third roll moment exists which is also dependent on α and γ . This moment is the Induced Roll Moment, $L(\gamma\alpha)$, and it may be added to the basic roll equation yielding:

$$L(\gamma\alpha) + L(\delta_A) + L(p) = I_x \dot{p} \quad (2)$$

where the moments written in stability coefficient form are:

$$L(\gamma\alpha) = C_{l_{\gamma\alpha}} \alpha (\sin 4\gamma) \frac{1}{2} \rho U^2 S d \quad (3)$$

$$L(\delta_A) = C_{l_{\delta_A}} \delta_A \frac{1}{2} \rho U^2 S d$$

$$L(p) = C_{l_p} \left(\frac{p d}{2U} \right) \frac{1}{2} \rho U^2 S d$$

In the case of wind tunnel Roll Lock-In where $\rho=0$ and α is constant, the basic roll equation becomes:

$$L(\delta_A) + L(\gamma\alpha) = 0 \quad (4)$$

Solving Eq.(4) for γ yields,

$$\gamma = \frac{1}{4} \sin^{-1} \left[- \frac{C_{l\delta_A} \delta_A}{C_{l\gamma\alpha} \alpha} \right] \quad (5)$$

From Fig. 9 we see that there are three possible cases.

In case 1, $L(\delta_A)$ is greater than $L(\gamma\alpha)$ for all values of γ and, thus, there is no value of α which can satisfy Eq.(4). Therefore the model will not lock-in and will roll.

In case 2, the two roll moments are equal and opposite at $\gamma = 67\frac{1}{2}^\circ$ and Eq.(4) is satisfied. The model will lock-in. This is seen to be the critical angle of attack.

In case 3, there are two values of γ which satisfy Eq.(4). First, for values in the range, $67\frac{1}{2}^\circ < \gamma \leq 90^\circ$, a static roll instability exists since a slight increase in γ yields a roll moment due to cant greater than the induced roll moment. This tends to cause a greater increase in γ and thus further static unbalance. If γ is slightly reduced a similar situation exists. Second, for values in the range, $45^\circ \leq \gamma \leq 67\frac{1}{2}^\circ$, a static stability exists and thus Roll Lock-In can occur in this range. Thus, for the wind tunnel case, the roll trim angle is given by Eq.(5) where $45^\circ \leq \gamma \leq 67\frac{1}{2}^\circ$.

In wind tunnel tests it is also noticed that the model, when excited, may have small oscillations in roll about the roll trim angle. These oscillations are either damping, constant amplitude, or undamping in nature. The frequency and stability of these oscillations may be predicted by assuming a linear variation of $L(\gamma\alpha)$ for the small γ range involved and by solving Eq.(2). Eq.(2) may be written as:

$$\ddot{\gamma} + N_1 \dot{\gamma} + N_2 \gamma = N_3 \quad (6)$$

where $N_1 = -\frac{1}{I_x} \left[C_{\ell p} \left(\frac{d}{2v} \right) \frac{1}{2} \rho v^2 S_d \right]$

$$N_2 = -\frac{1}{I_x} \left[\tilde{C}_{\ell \gamma \alpha} \propto \frac{1}{2} \rho v^2 S_d \right]$$

$$N_3 = +\frac{1}{I_x} \left[C_{\ell \delta_A} \delta_A \frac{1}{2} \rho v S_d \right]$$

where $\tilde{C}_{\ell \gamma \alpha}$ = local slope of the induced roll moment curve at $\alpha = \text{const.}$ The general solution to Eq. (4) is given by:

$$\gamma = K_1 e^{\phi_1 t} + K_2 e^{\phi_2 t} + K_3 \quad (7)$$

where

$$\phi_{1,2} = \lambda_{1,2} + i \omega_{1,2} = -\frac{N_1}{2} \pm \frac{1}{2} \sqrt{N_1^2 - 4N_2}$$

$$K_{1,2} = \frac{\dot{\gamma}_0 - \phi_{2,1} \gamma_0 + K_3 \phi_{2,1}}{\phi_{1,2} - \phi_{2,1}}$$

$$K_3 = \frac{N_3}{N_2}$$

The frequency (ω) of the roll oscillations is given by:

$$\omega_{1,2} \approx \pm \left(-\frac{1}{I_x} \tilde{C}_{\ell \gamma \alpha} \frac{1}{2} \rho v^2 S_d \right)^{1/2} \equiv \omega \quad (8)$$

and the damping by:

$$\lambda_{1,2} \approx \frac{1}{2 I_x} \left(C_{\ell p} \frac{d}{2v} \frac{1}{2} \rho v^2 S_d \right) \equiv \lambda \quad (9)$$

Now Eq. (7) may also be written as

$$\gamma = \gamma_T + B e^{\lambda t} \cos(\omega t + \delta) \quad (10)$$

where

$$\gamma_T = \text{Roll Trim Angle}$$

Thus we see from this development that the introduction of the non-linear Induced Roll Moment into the classical linear roll theory provides an explanation for and a prediction of Roll Lock-In and its dynamic stability.

It now remains to determine (1) how well this Roll Lock-In Theory is able to represent the actual motion, and (2) how accurately the various aerodynamic stability coefficients may be determined from the experimental motion by using the theory.

DATA REDUCTION AND RESULTS

The Roll Lock-In Theory, Eq.(10), was fitted to the roll angle data, $\gamma(t)$, by using the Method of Differential Corrections. This reduction technique was developed by Professor Eikenberry at the University of Notre Dame⁸.

Basic Finner

Two Basic Finner Roll Lock-In motions were reduced⁹. In one motion, the roll oscillations damped, Fig.10. In the other motion, the roll oscillations undamped, Fig.11. The constants of these two motions as determined by the application of the Method of Differential Corrections are given in Fig.12.

Two important findings stand out. First, the Roll Lock-In Theory represents the rolling motion with good accuracy since the Probable Errors of "Fit" are 1.49° for the damped motion and 1.69° for the undamped motions. Second, we note that all of the roll constants are quite well determined as seen from their Probable Errors.

The aerodynamic stability derivatives are given in Fig.13 together with the important Roll Trim Angle.

In the undamped case C_{ℓ_p} is small and positive. The % P.E. is misleading in this case.

Aerobee Fins

The rolling motion of an Aerobee Fins model was also reduced¹⁰. The motion is shown in Fig.14. The constants of this motion as obtained from the "fit" are given in Fig.15. We note that the Roll Lock-In Theory represents the motion to an accuracy of 1.875° and that, again, all of the constants are very well determined.

Aerobee 350

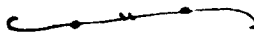
The rolling motions of the Aerobee 350 were quite unexpected. First, Roll Lock-In occurred at extremely small angles of attack, and, second, the stability of the motions was highly variable, Fig.16. Fig.17 contains values of the Roll Trim Angle over various portions of the motion shown in Fig.17 (X105) and, also, for two other test runs.

DISCUSSION

The primary purpose of this study was to determine if Roll Lock-In exists at supersonic speeds. The rolling motions obtained from the Free Rolling Wind Tunnel Technique, developed in this study, revealed that Roll Lock-In does exist on three different missile configurations at supersonic speeds. The data also suggests that Roll Lock-In should be considered a real possibility for any fin stabilized configuration at an angle of attack at supersonic speeds.

The Free Rolling Wind Tunnel Technique has also yielded an accurate determination of the important Roll Lock-In angle. This angle is important because the Side Moment critically depends on this angle. The Side Moment directly determines the size of Catastrophic Yaw.²

The Roll Lock-In Theory has been "fitted" to the experimental roll data and found to represent the transient free oscillating rolling motion to an accuracy of less than $\pm 2^\circ$. Also, it has been found possible to determine accurate values for the Induced Roll Moment Stability Coefficient and for the Roll Damping Moment Stability Coefficient for the Basic Finner model and for the Aerobee Fins Only Model.



While the observed rolling motions were generally in accordance with theoretical expectations and while the associated stability coefficients were well determined in a number of cases, some unexpected and quite unusual rolling motions were obtained which require consideration and discussion.

As seen in Figs. 10 and 11, the basic Roll Lock-In motion is a simple sine wave about a constant roll trim angle. The motion may damp or undamp. However, in Figs. 18-20 we see examples of serious departures from this basic motion.

In Fig. 18, we note that the Roll Trim Angle on a model of the Aerobee rocket appears to change with time. This characteristic may be due to the non-linear nature of the induced roll moment with roll orientation. More specifically, it may be that the average magnitude of the difference between the instantaneous roll angle and the roll trim angle is the critical parameter. As the size of the average magnitude decreases, the true linear case is reached and a constant value of

roll trim is obtained.

The dynamic stability of the roll oscillations may also depend on the average magnitude of the roll angles during an oscillation. In Figs. 16 and 19, we see the model "hunting" different roll trim angles. In Fig. 19, roll trim angles of approximately, 40° , 135° , and 225° are sought. These roll trim angles are approximately 90° apart as expected from the Roll Lock-In theory for a four finned missile. However, it is difficult to understand why the missile "hunts" for a roll trim angle.

One simple reason may be poor wind tunnel flow. During the tests at Notre Dame we were able to influence the dynamic stability of Roll Lock-In by introducing a disturbance in the throat of the nozzle of the wind tunnel. However, when the disturbance was present, Fig. 8, the rolling motion stayed at one roll trim, rather than "hunting". One would have expected the opposite. Thus, "hunting" may be a real characteristic.

One possible explanation may be found in considering non-linearities in the dynamic stability. For large amplitude oscillations, the motion may be dynamically stable and for small amplitudes dynamically unstable. The variation in roll trim angle, increasing or decreasing, may be an important factor.

The rolling motion from one test of the Aerobee Rocket Model is shown in Fig. 20. In Fig. 20a the roll oscillations damp during the interval from 275 sec. to 475 sec. However at 475 sec. the oscillations begin to undamp and at 675 sec. the model begins rolling with a negative velocity. This rolling velocity portion is shown in Fig. 20b. In Fig. 20c this rolling velocity reduces and the model locks in at a new roll trim position.

In some tests both positive and negative steady rolling velocities have been observed.

During the tests it was sometimes noted that the Aerobee model tended to select a particular one of the four possible roll lock-in angles. That is to say, the model seemed to prefer to trim in roll near one particular fin. Inspection of the model suggested that the four fins were not all of the exact same size. It was therefore felt that the Roll Lock-In Theory should be extended to include differences in fin size. More specifically, it could be assumed that one fin was larger than the other three and, thus, a new roll moment could be added. We shall call this new roll moment the Transverse Area Roll Moment. It is given by

$$L_{\delta, \alpha} \delta, \alpha = C_{L, \delta, \alpha} \delta (\sin \alpha) \frac{1}{2} \rho U^2 S d$$

Also, during the rolling tests it was noted that center of gravity of the model was not precisely on the axis of roll. Therefore, it seemed desirable to introduce an additional roll moment due to cg offset. We shall call this new roll moment, the Transverse C.G. Roll Moment. It has the same form as the Transverse Area Roll Moment since it also varies once per revolution.

$$L_r(hm) = hmg \sin \delta$$

When these two moments are introduced the modified Roll Lock-In Theory becomes,

$$L(\delta_a) + L(p) + L(\gamma_a) + L(\gamma, \alpha) + L(hm) = I_x \dot{p}$$

For the wind tunnel case where α is a constant and the transient rolling motion has damped ($\dot{p} = p = 0$), we may solve for the new Roll Trim Angle. Here we find that the model will, in fact, prefer one fin orientation to the other three. Special model designs and tests should be carried out to study this motion and its dynamic stability.

The tests on the Aerobee Fin only model were of special importance. When Roll Lock-In was first seen at subsonic speeds on bomb models and the Basic Finner, it was felt that vortices shedding from the body were acting on the fins so as to cause Roll Lock-In¹². Special tests were run to explore this idea. When cruciform fins alone were tested they demonstrated Roll Lock-In. Since there was no body, body vortices certainly do not offer an explanation.

Unfortunately, there continues to exist a widespread feeling that body vortices are essential to Roll Lock-In. Thus, in studying the Aerobee Rocket, it was felt desirable to demonstrate that Roll Lock-In can occur when no body exists. The rolling motions in Figs. 8 and 19 clearly confirm the crucial significance of the fins.

In seeking cures or "fixes" for Roll Lock-In, it is suggested that Fin Only configurations be studied. Some promising results have already been obtained at Notre Dame in the area.

CONCLUSIONS

It is concluded that:

1. Roll Lock-In can exist at supersonic speeds on the Aerobee Rocket and the Basic Finner,
2. The cause of Roll Lock-In on the Aerobee Rocket is due to the fin design,
3. The Roll Lock-In Theory accurately represents the rolling motion,
4. The Roll Trim Angle, the Induced Roll Moment Stability Coefficient, and the Roll Damping Moment Stability Coefficient may be accurately determined by "fitting" the Roll Lock-In Theory to the experimental data obtained from the Free Rolling Wind Tunnel Technique,
5. The Modified Roll Lock-In Theory offers a means of predicting the affects of transverse area and transverse mass,
6. Catastrophic Yaw may be expected in the Aerobee Rocket and other sounding rockets.

REFERENCES

1. Nicolaides, John D. , On the Free Flight Motion of Missiles Having Slight Configurational Asymmetries, BRL Rpt. No. 858, 1953, and IAS Preprint No. 395, 1952.
2. Nicolaides, John D. , Two Non-Linear Problems in the Flight Dynamics of Modern Ballistic Missiles, IAS Report No. 59-17, 1959.
3. Nicolaides, John D. , Missile Flight and Astrodynamics, TN 100A, Bureau of Naval Weapons, 1961.
4. Stone, George W. , The Aerodynamic Stability of a Coasting Vehicle During High-Speed Exit From the Atmosphere, SC-TM-65-58A, Sandia Laboratory, 1965.
5. Nicolaides, John D. and Eikenberry, Robert S. , Dynamic Wind Tunnel Testing Techniques , AIAA Paper No. 66-752, 1966.
6. Nicolaides, John D. , Eikenberry, Robert S. , and Ingram, Charles W. , The Determination of Aerodynamic Stability Coefficients from Sounding Rocket Flight Data, AIAA Paper, Sounding Rocket Vehicle Technology Specialists Conference, February 1967.
7. Rhodes, C. W. and Shannon, J. H. W. , Results and Conclusions of the Joint R. A. E. /W. R. E. Research Programme on the Flight Dynamics and Ballistic Consistency of Freely Falling Missiles: Part I Bombs Stabilized by Fixed Cruciform Fins, Department of Supply, Australian Defense Scientific Service, Weapons Research Establishment, HSA 20, 1965.
8. Eikenberry, R. S. , Wobble, A Computer Program for the Analysis of Quadracyclic Missile Motions, Aero-Space Engineering Department, University of Notre Dame, (In preparation).
9. Nelson, R. C. , On the Pure Pitching Motion of the Basic Finner Missile, Aero-Space Engineering Department, University of Notre Dame, 1966.
10. Siddons, W. D. , Jr. , Aerobee Lock-In Fins Only Configuration. Report-Department of Aero-Space Engineering, University of Notre Dame, 1966.

11. Bozzonetti, E. R., Jr., Analysis of the Oscillatory Motions Associated with Roll Lock-In. Report-Department of Aero-Space Engineering, University of Notre Dame, 1966.
12. Griffin, T. F., and R. Heald, On the Pure Rolling Motion of the Low Drag Bomb at Large and Small Angles of Attack, Department of the Navy, Ballistic Technical Note No. 19, Washington, D. C., 1956.

SYMBOLS

α	Angle of Attack
γ	Angle of Roll Orientation
p	Rolling Velocity
V	Velocity
ρ	Air Density
S	Reference Area
d	Diameter
I_x	Axial Moment of Inertia
$L(\delta_A)$	Roll Moment Due to Fin Cant
$L(p)$	Roll Damping Moment
$L(\gamma\alpha)$	Induced Roll Moment
$C_{l\delta_A}$	Roll Moment Coefficient Due to Fin Cant
C_{lp}	Roll Damping Moment Coefficient
$C_{l\gamma\alpha}$	Induced Roll Moment Coefficient
t	Time
ST	Fitted Slant of Trim Axis per Unit Time
B	Fitted Initial Amplitude
γ_T	Roll Trim Angle
ω	Angular Frequency
λ	Damping Rate
δ	Phase Angle

$\tilde{C}_{l\dot{\phi}}\alpha$

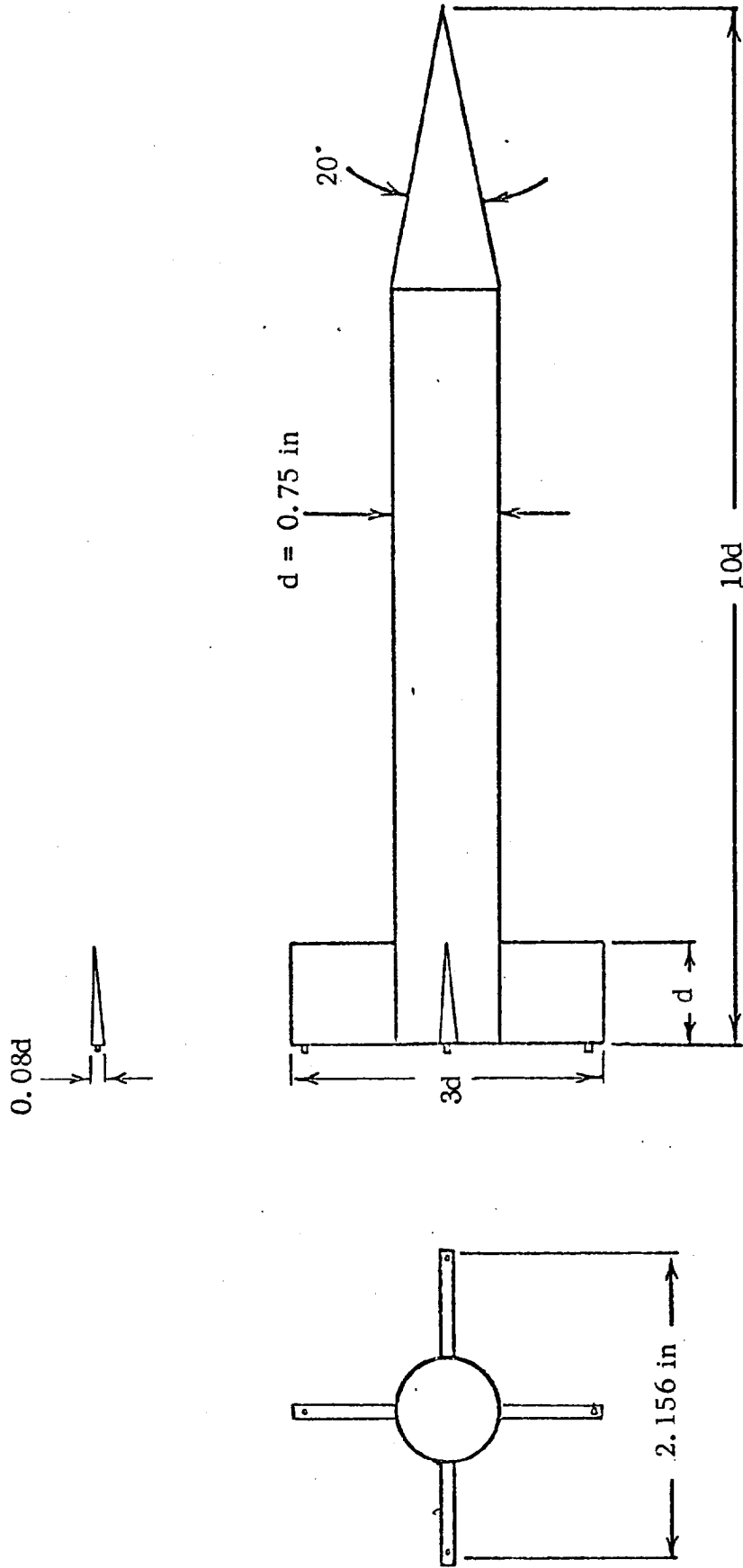
Local Slope of the Induced Roll Moment
Coefficient at Constant α

ϕ

Roll Angle

$\dot{\phi}$

Roll Acceleration



BASIC FINNER MODEL
FIGURE 1

AEROBEE 350 MODEL

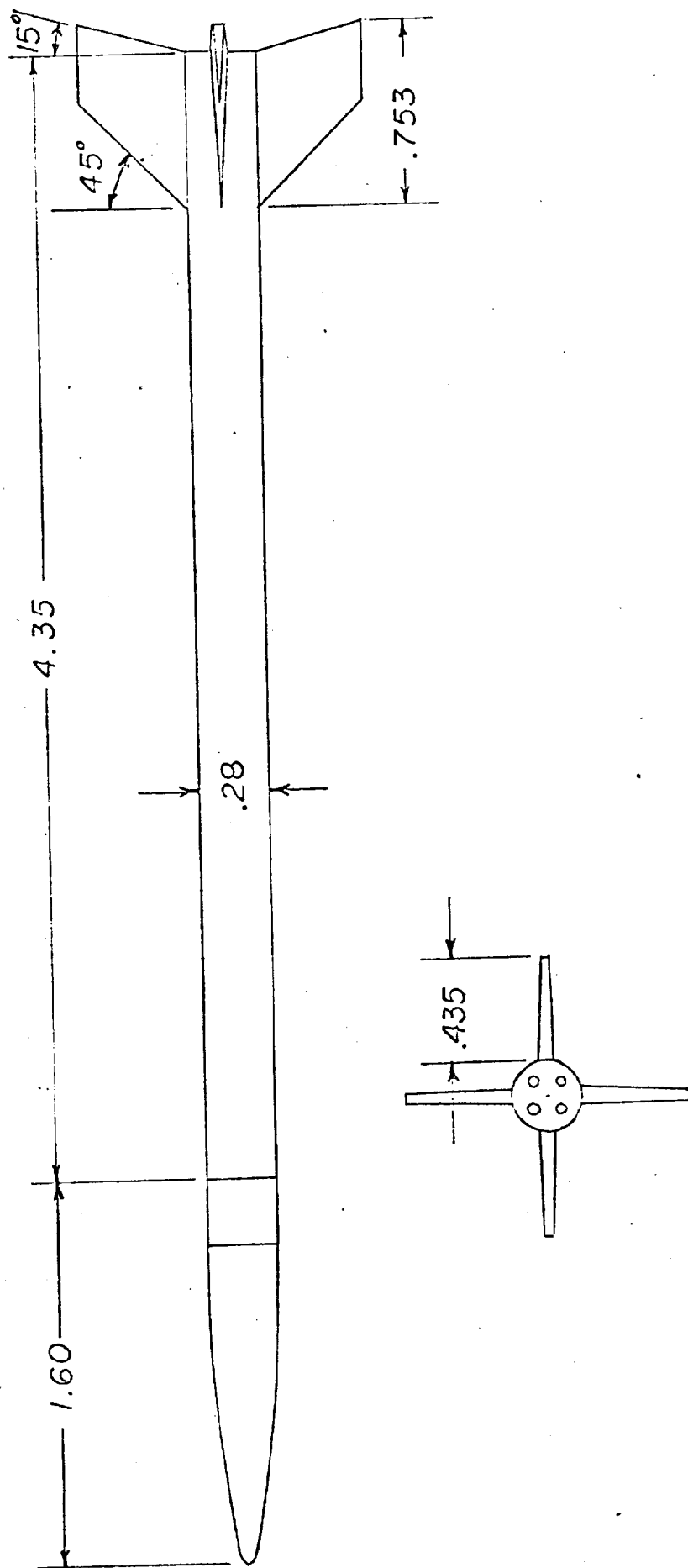


FIGURE 2

AEROBEE "FINS ONLY" MODEL

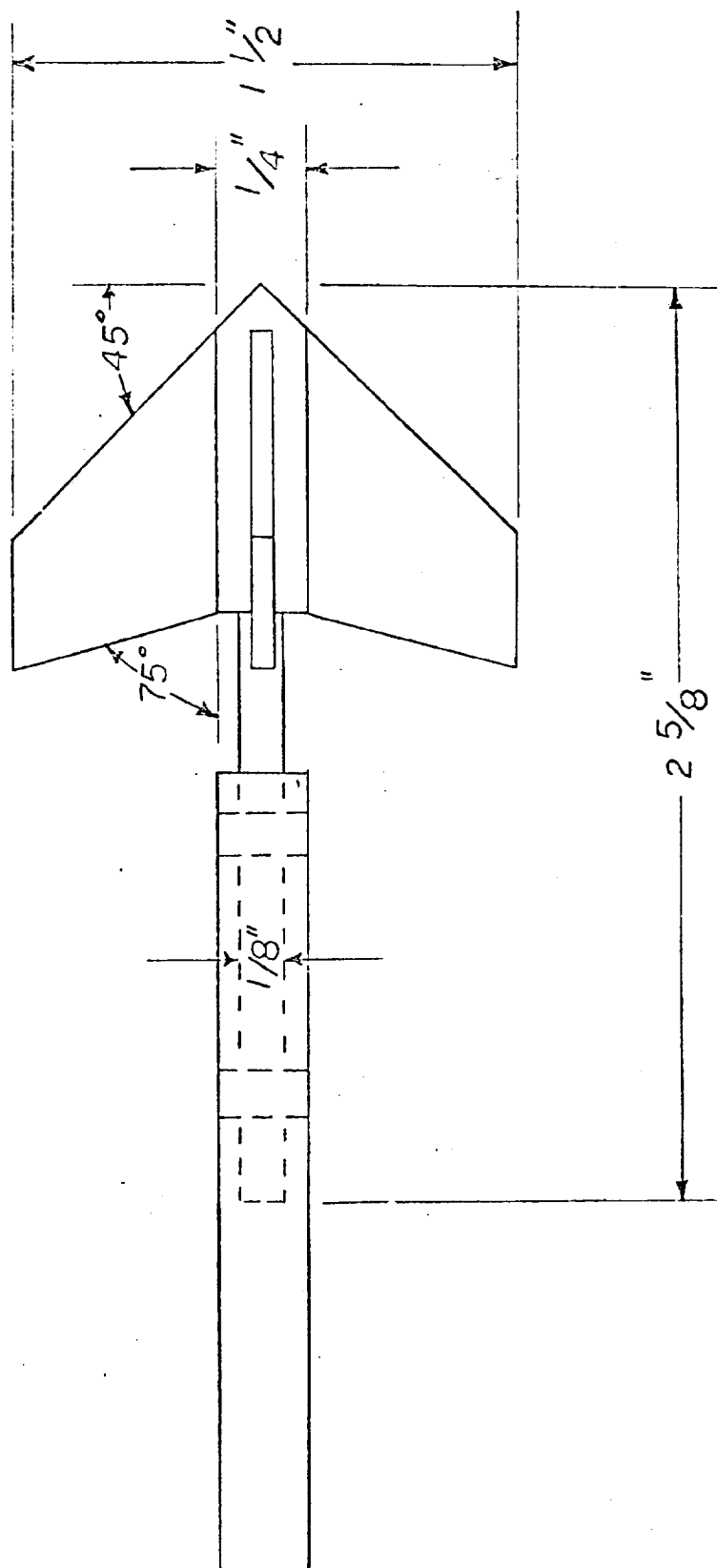
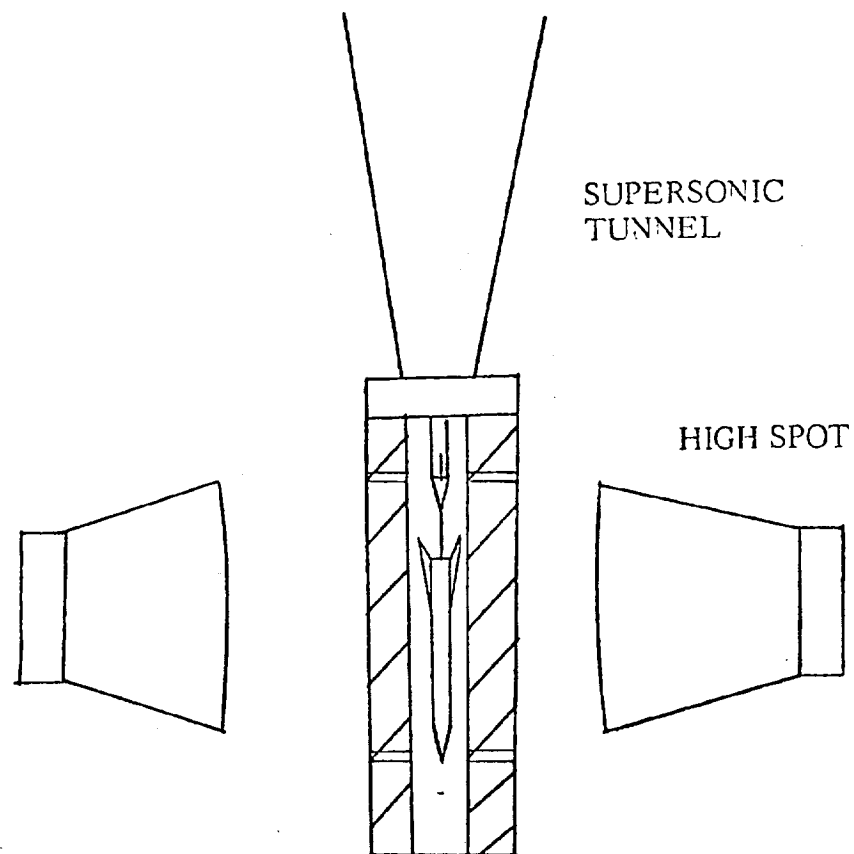
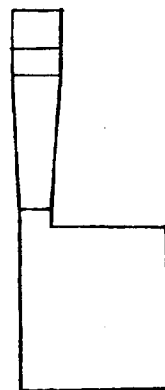


FIGURE 3



FASTAX
CAMERA



GOOSE

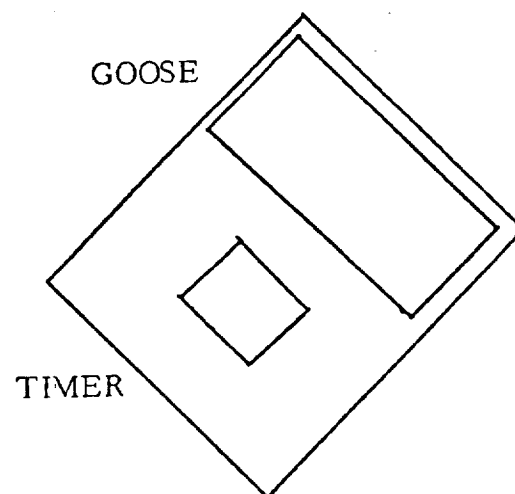


FIGURE 4

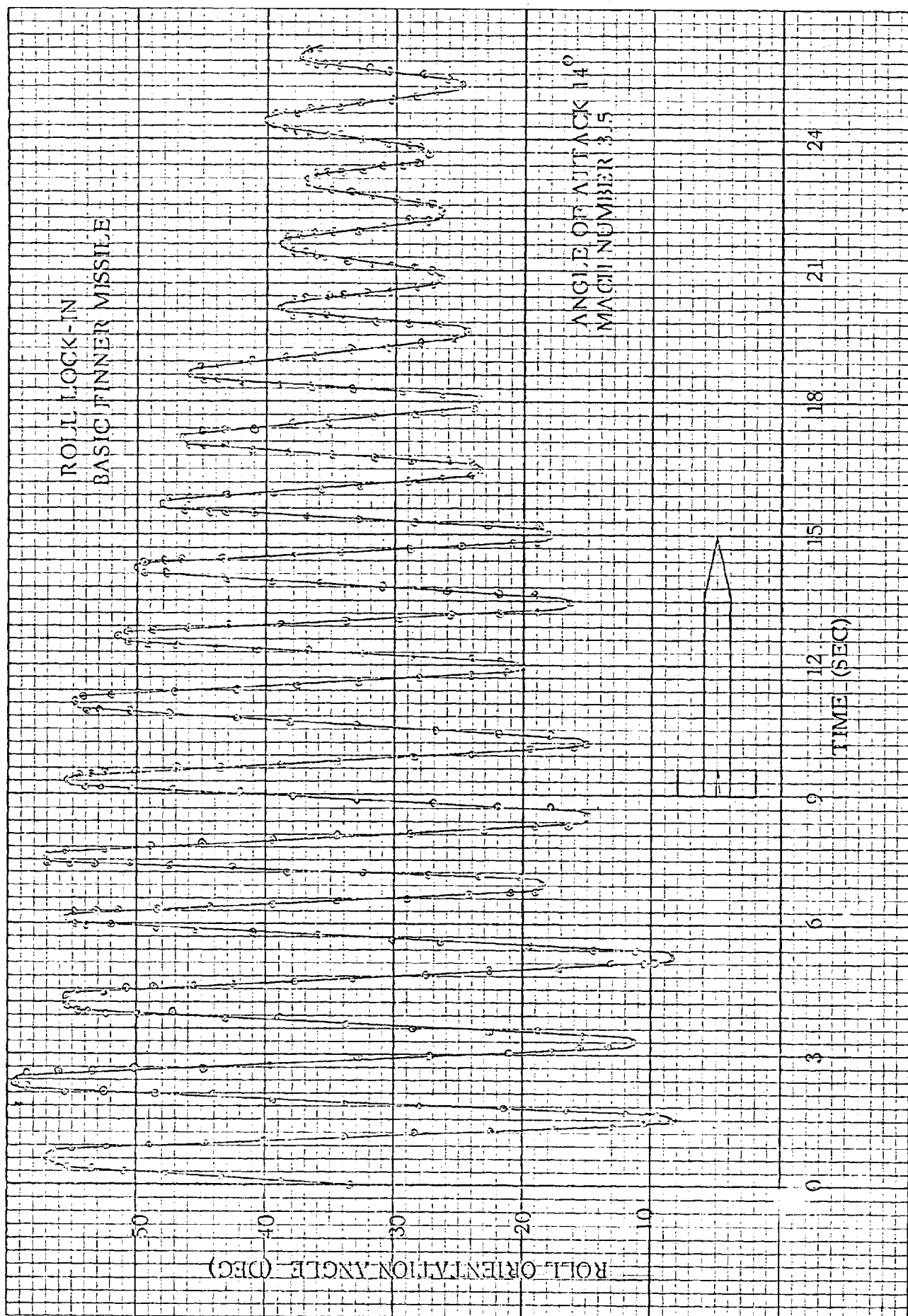
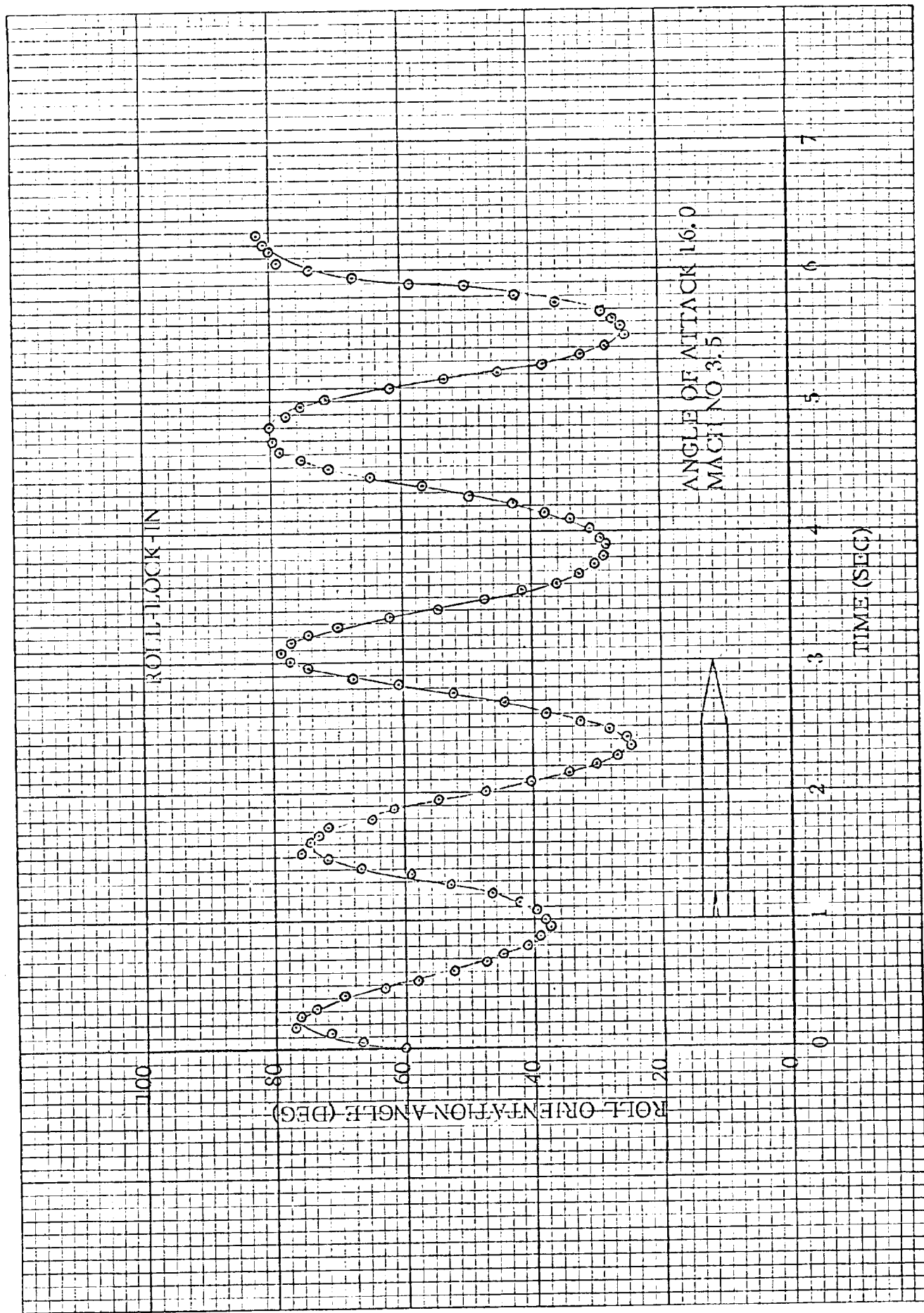


FIGURE 5



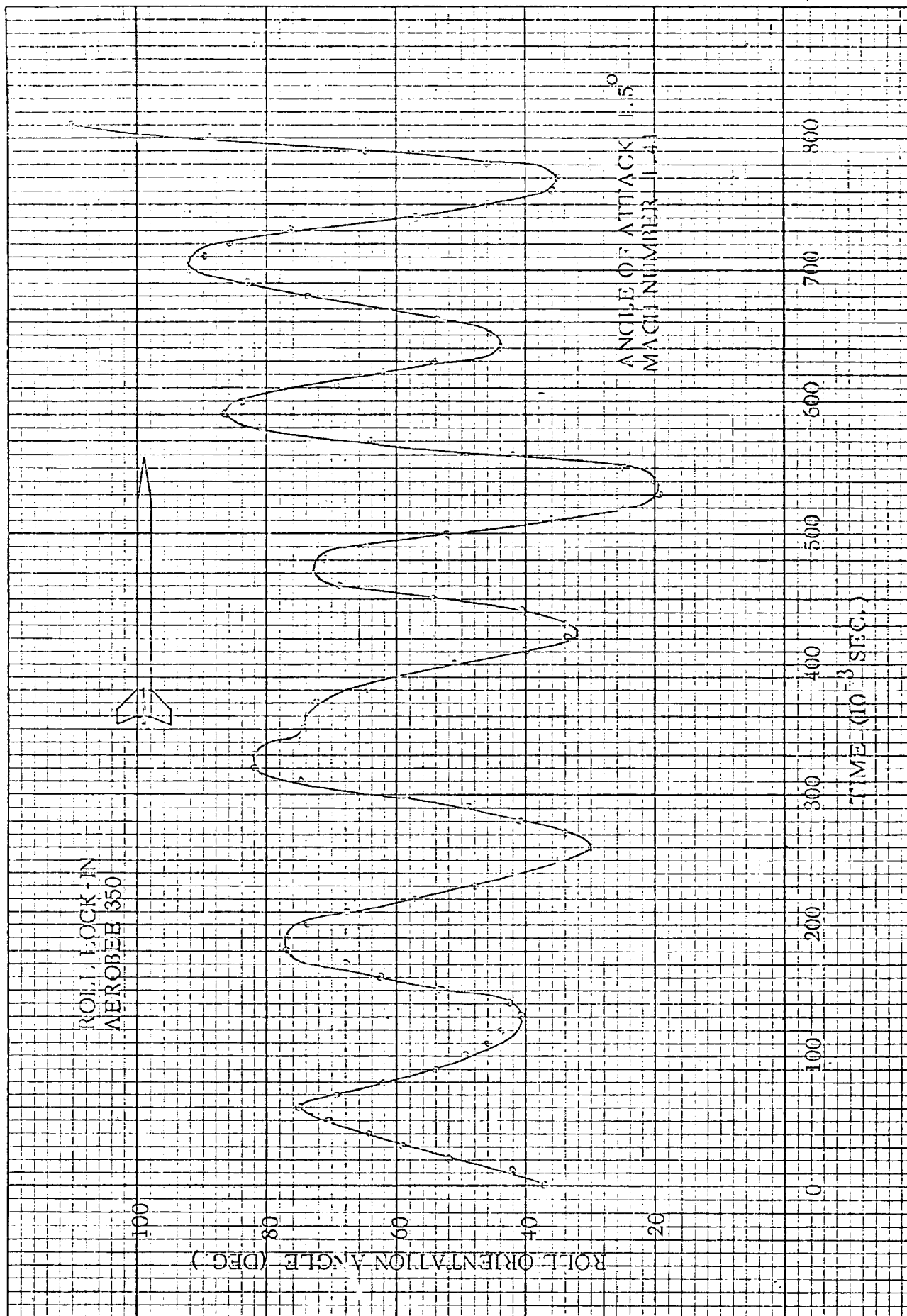


FIGURE 7

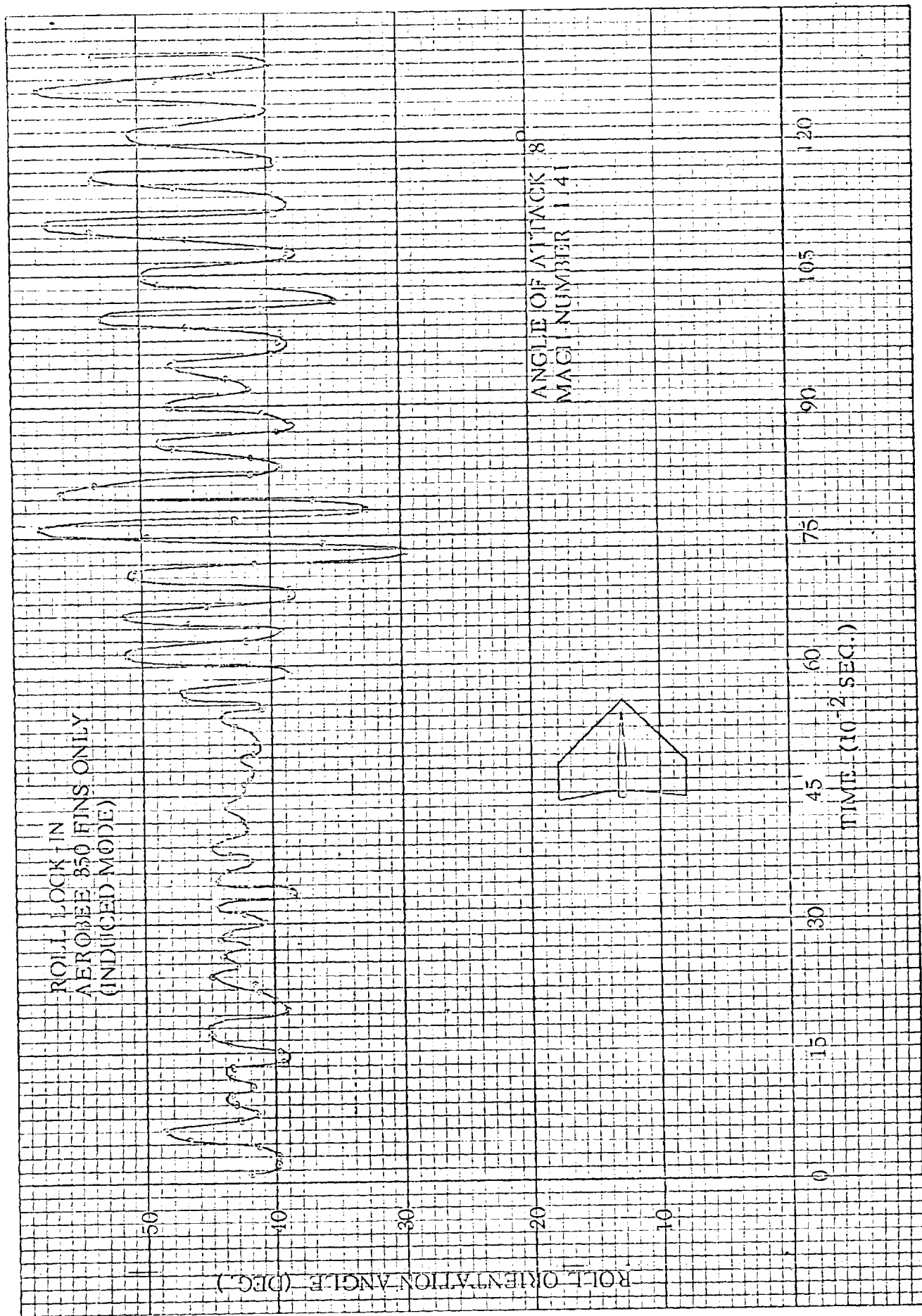


FIGURE 8

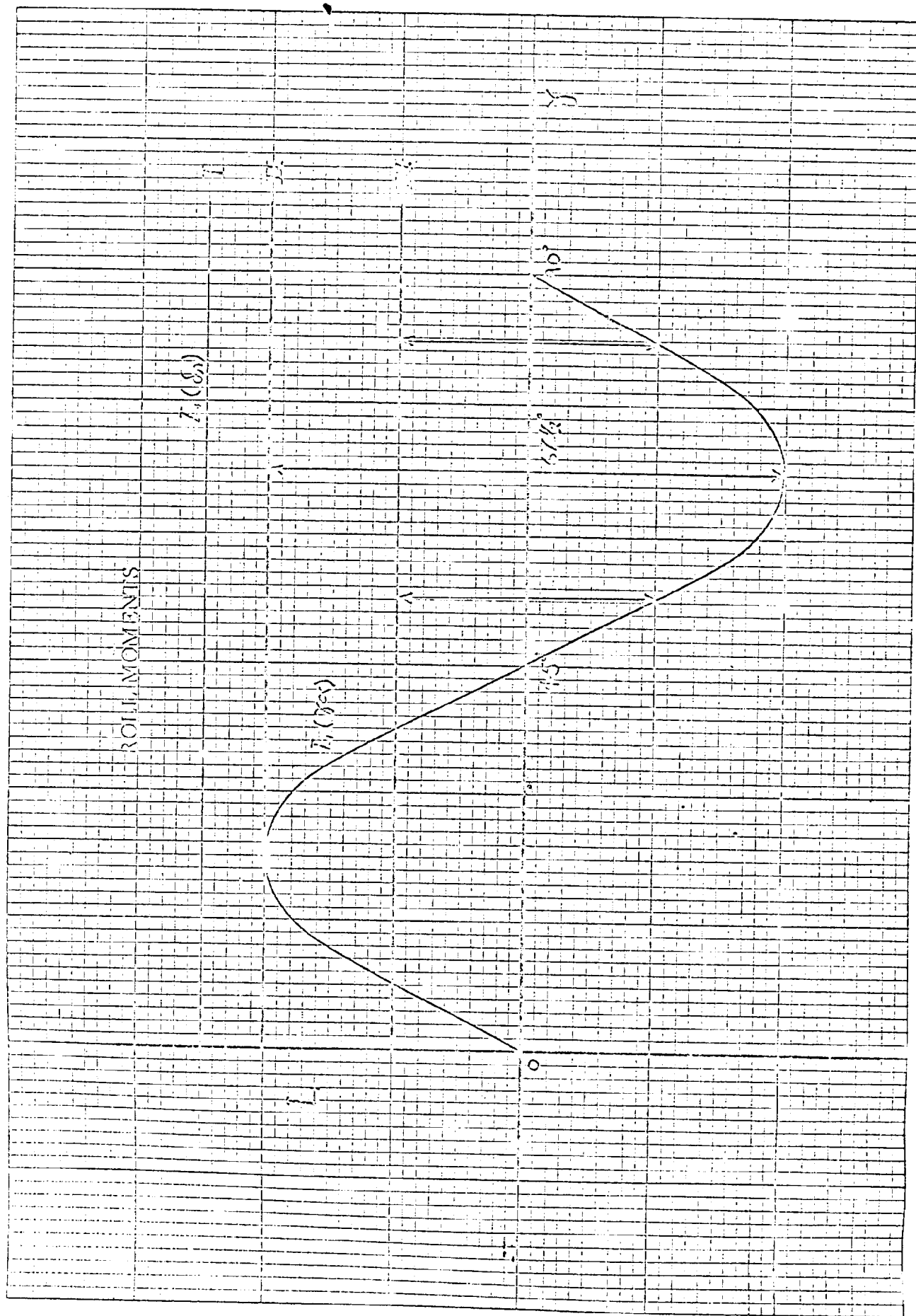


FIGURE 9

FREDERICK POST COMPANY
301 TR10 CROSS SECTION 10 X 10 PER INCH

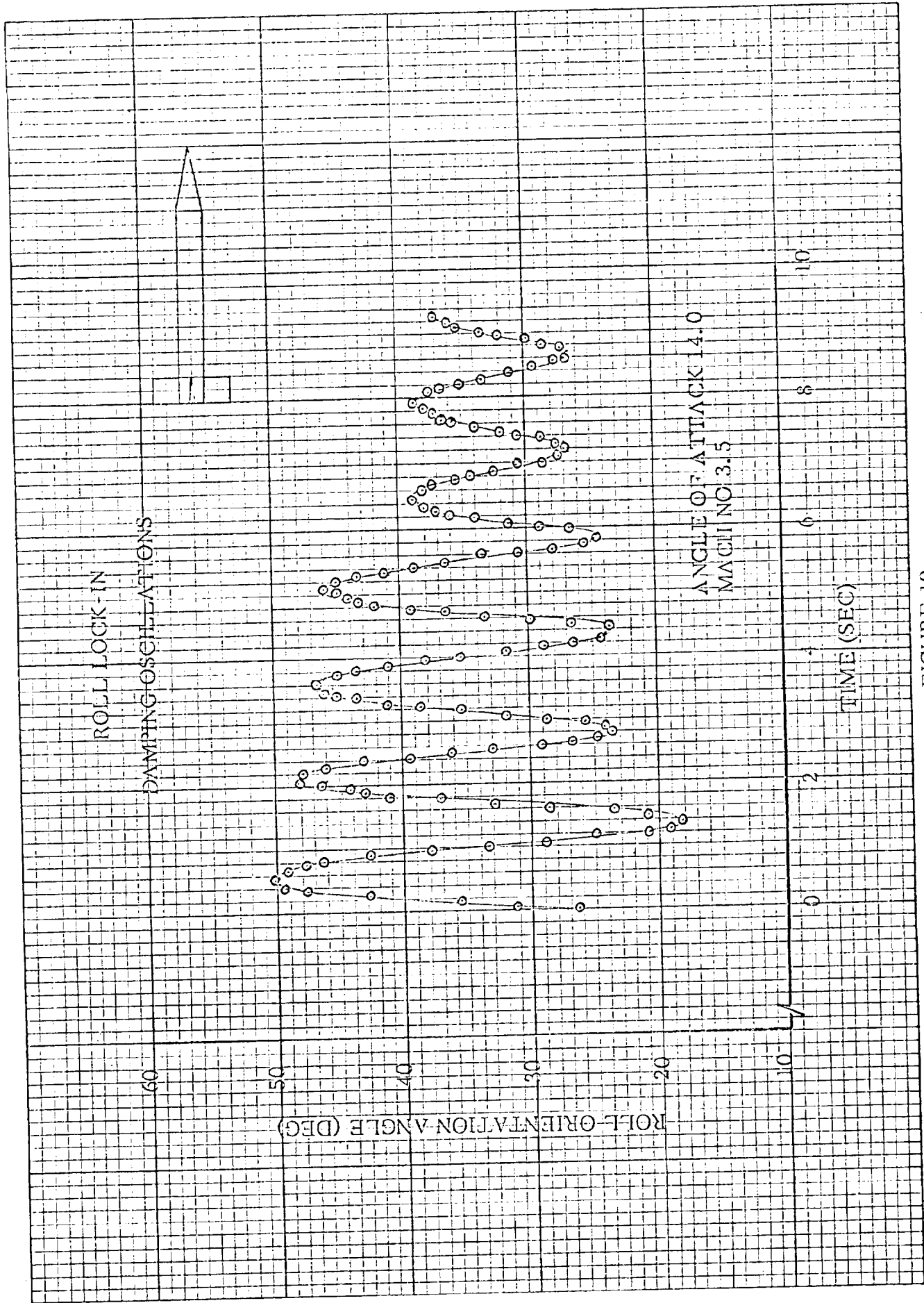


FIGURE 10

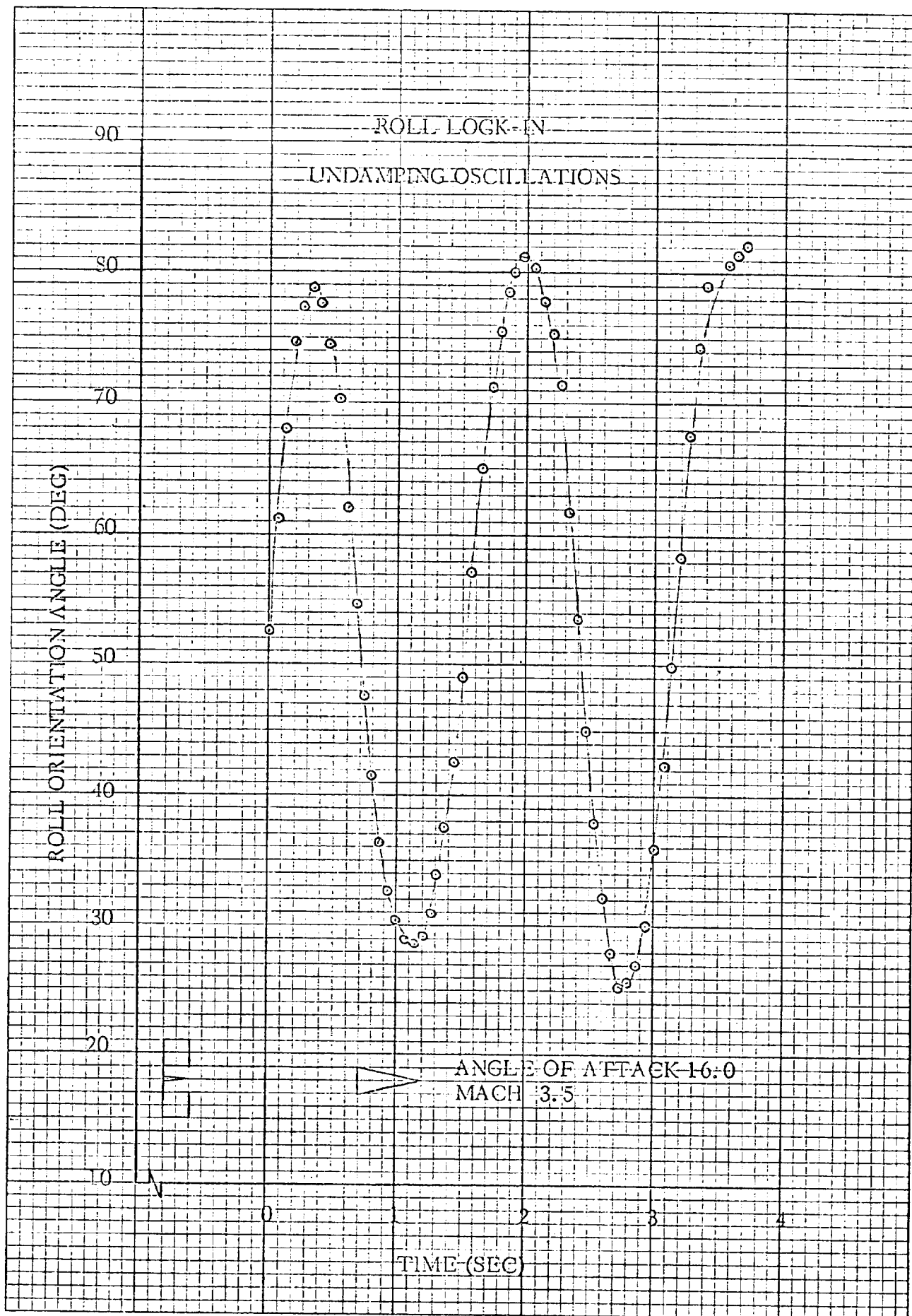


FIGURE 11

BASIC FINNER
CONSTANTS FROM COMPUTER FIT

<u>Damping Mode</u>					
γ_T	S_T	B	λ	ω	δ
(Deg)	(Deg/Sec)	(Deg)	(Sec-1)	(Rad/Sec)	(Rad)
37.1	-.416	17.5	-.135	4.25	3.78
P.E. .255	.047	.482	.0073	.0071	.026
<u>Undamping Mode</u>					
49.3	2.08	26.2	.023	3.86	4.73
P.E. .507	.240	.693	.0115	.0113	.024

FIGURE 12

BASIC FINNER
AERODYNAMIC DATA

	<u>Damping</u>		<u>Undamping</u>	
	Value	% Error	Value	% Error
γ_T	37.1°	0.687	49.3°	1.029
$C_{l\gamma\alpha}$	-0.027	0.1646	-0.019	0.285
C_{lp}	-6.66	0.518,	1.11	47.8

FIGURE 13

EFFICIENCY® LINE NO. 988
CROSS SECTION - 10 SQUARES TO INCH

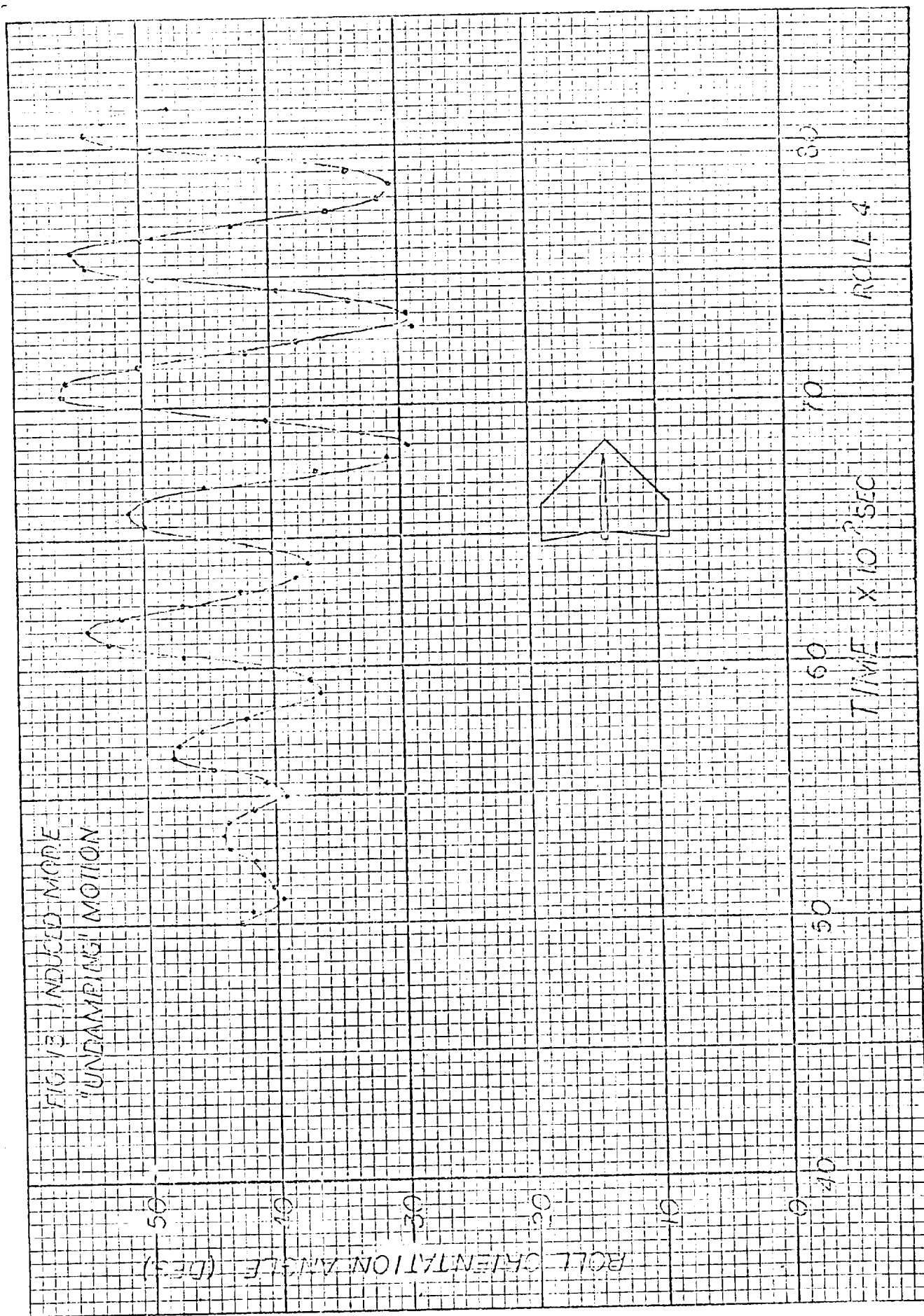


FIGURE 14

AERO-BEE "FINS ONLY"

Parameter	Value	Probable Error
γ_T	43.784 ⁰	0.507 ⁰
S_T	-8.361 ⁰	3.335 ⁰
λ	3.212	0.492
ω	130.717	0.468
B	6.409	0.578
δ	4.244	0.086
Sum of residuals squared	364.0	1.875
Probable error of fit	1.875 ⁰	

FIGURE 15

KILDEMECK POST COMPANY
501 TRIO CROSS SECTION 10 X 10 PER INCH

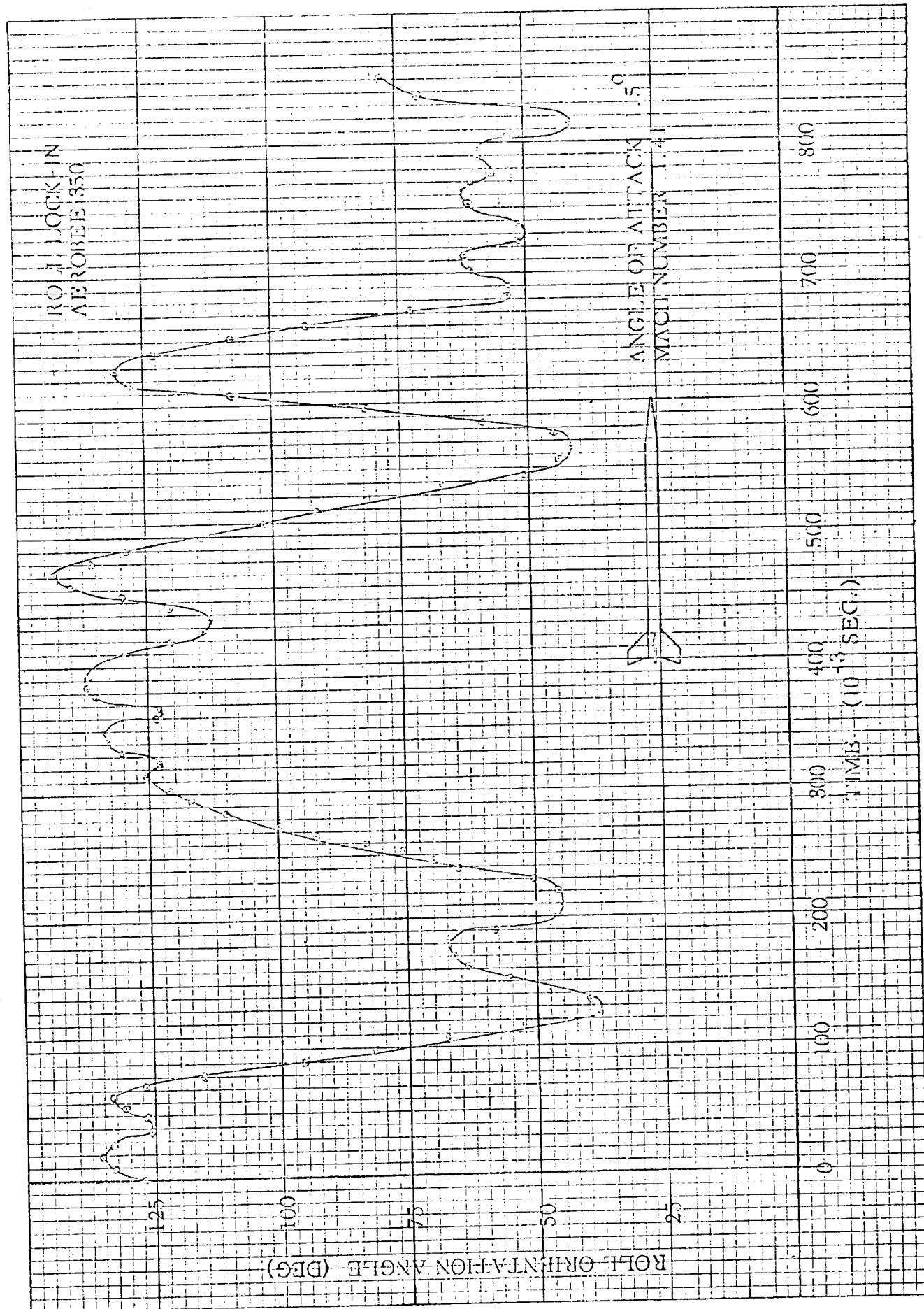
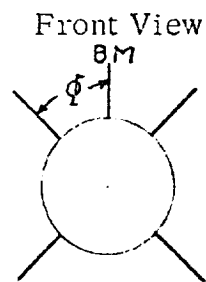


FIGURE 16

AEROBEE 350

Rolling Trim Angle Data



Film	Time Interval (10^{-3} Sec)	ϕ
X105	0-100	41.0°
	100-250	53.0°
	250-550	38.0°
	550-850	58.0°
X107	0-350	47.0°
	350-700	52.0°
	850-1350	78.5°
	1350-1800	30.5°
	1950-2500	47.0°
X118	0-650	59.0°

FIGURE 17

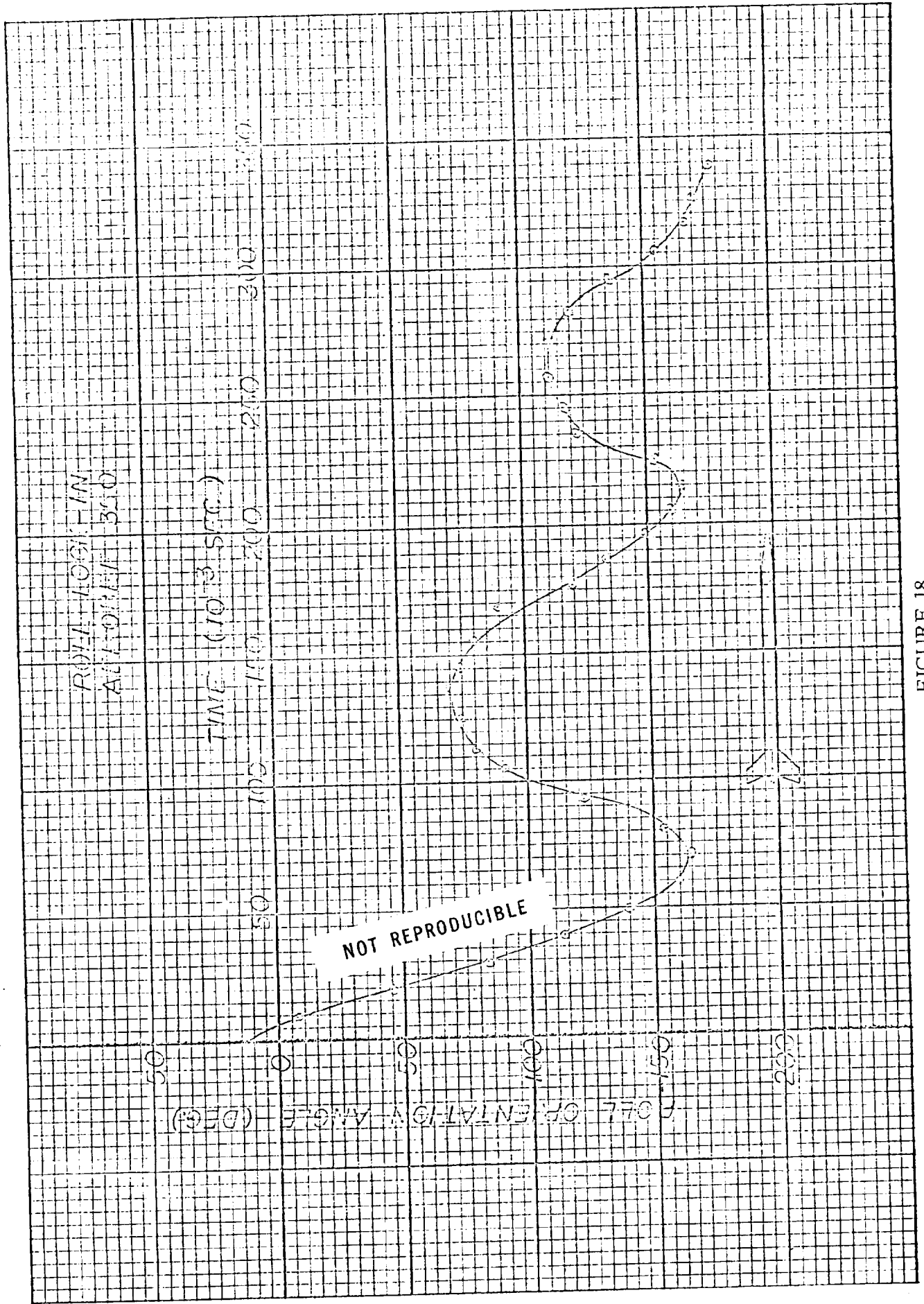
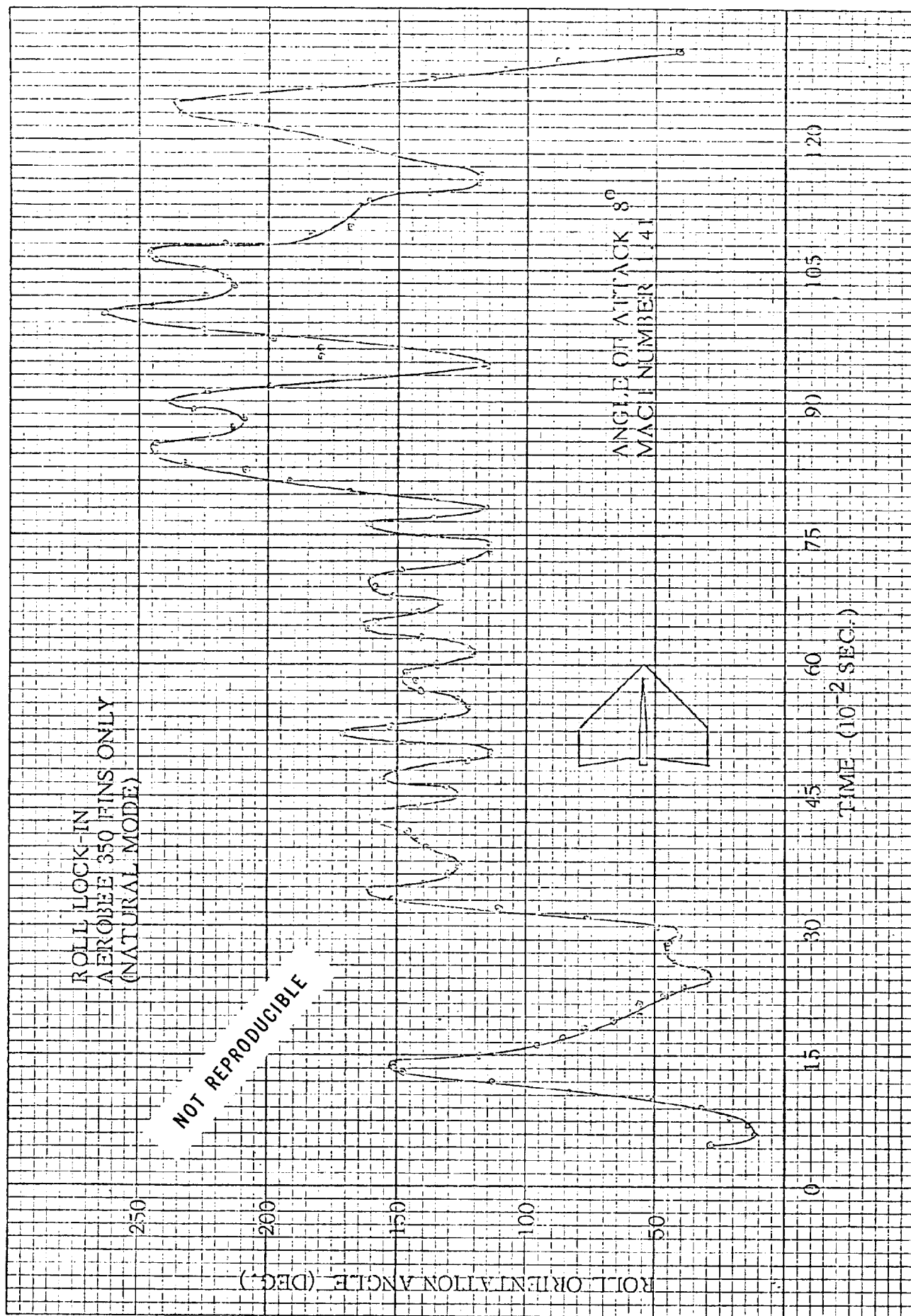


FIGURE 18



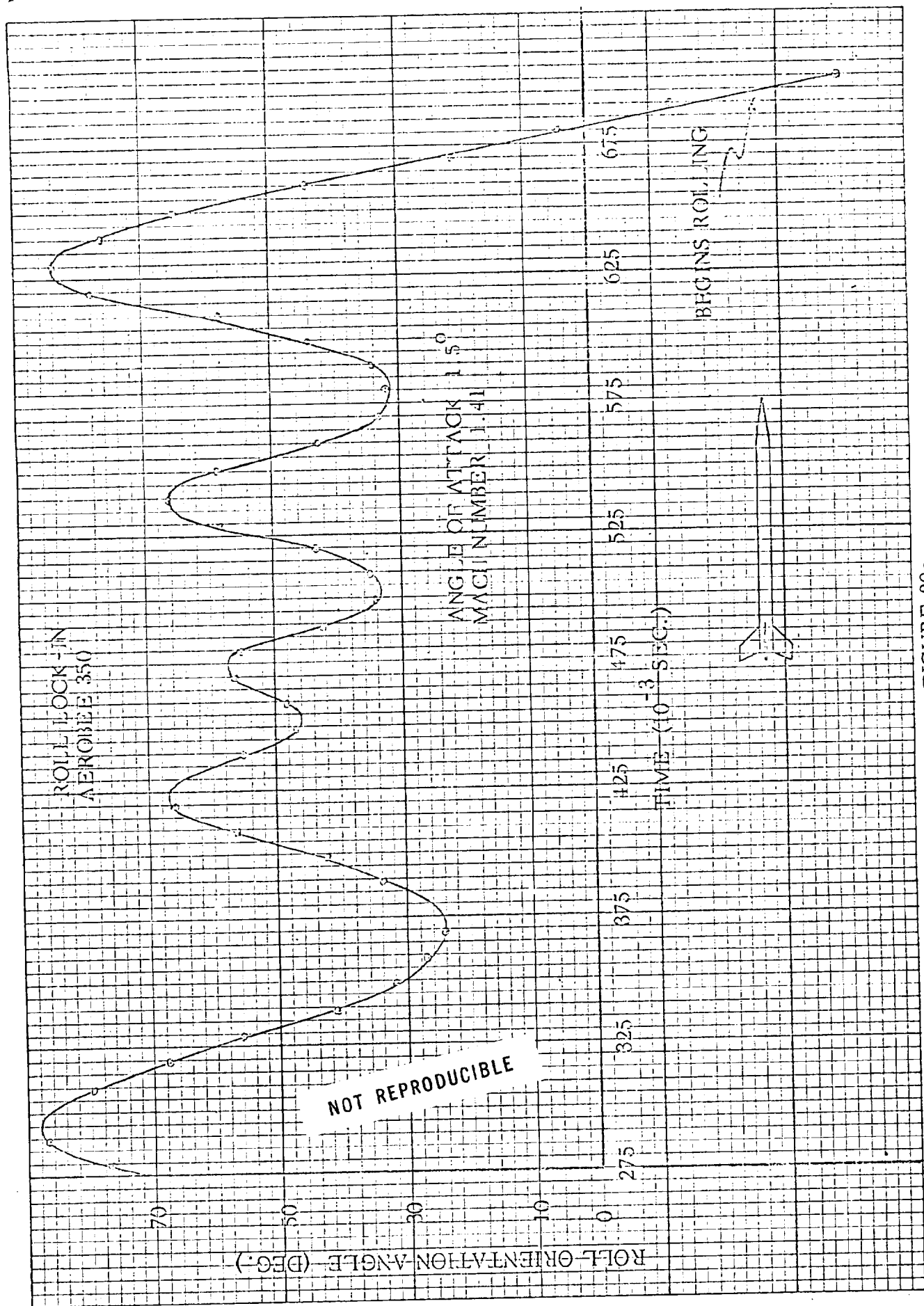
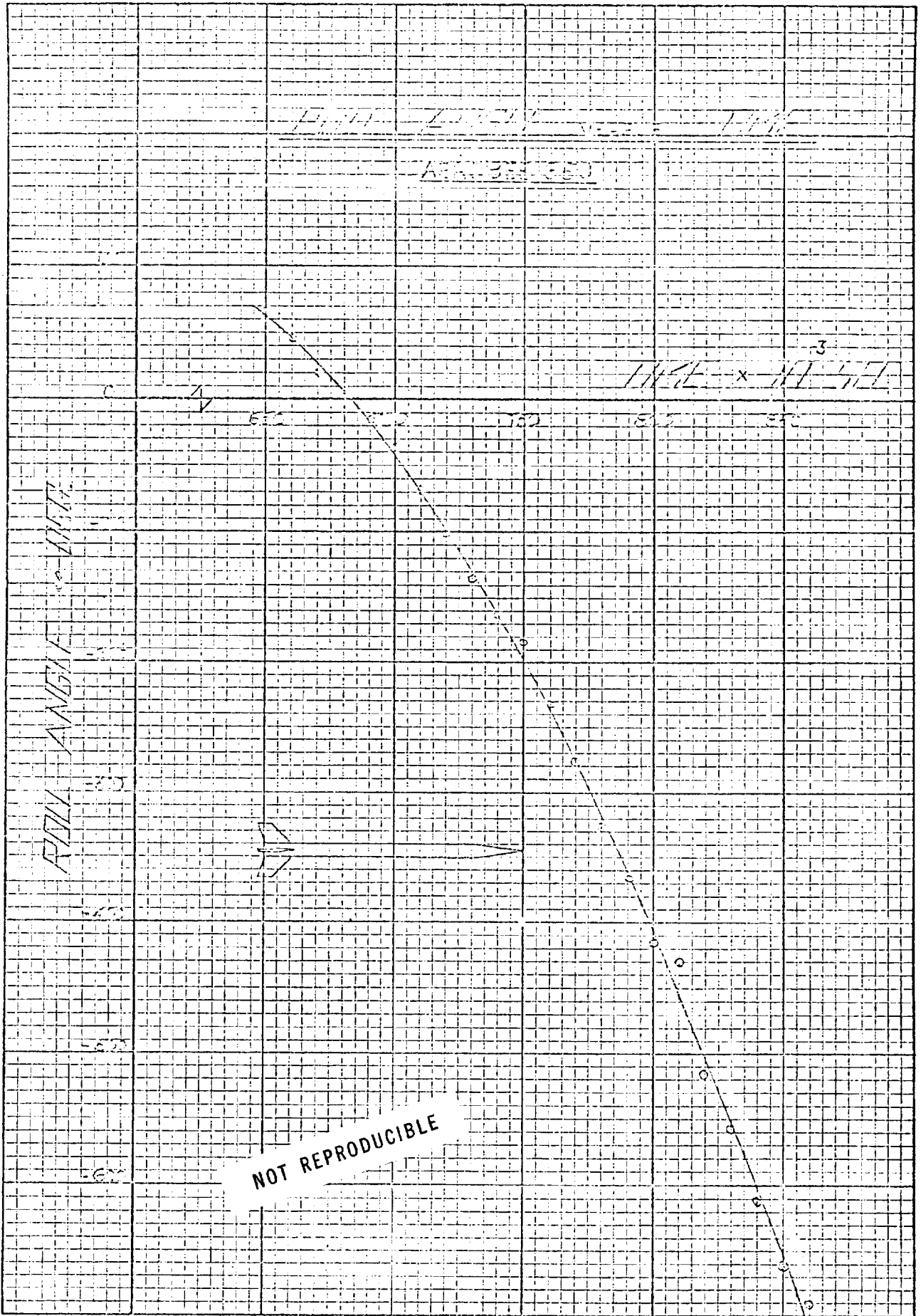


FIGURE 20a



NOT REPRODUCIBLE

FIGURE 20b

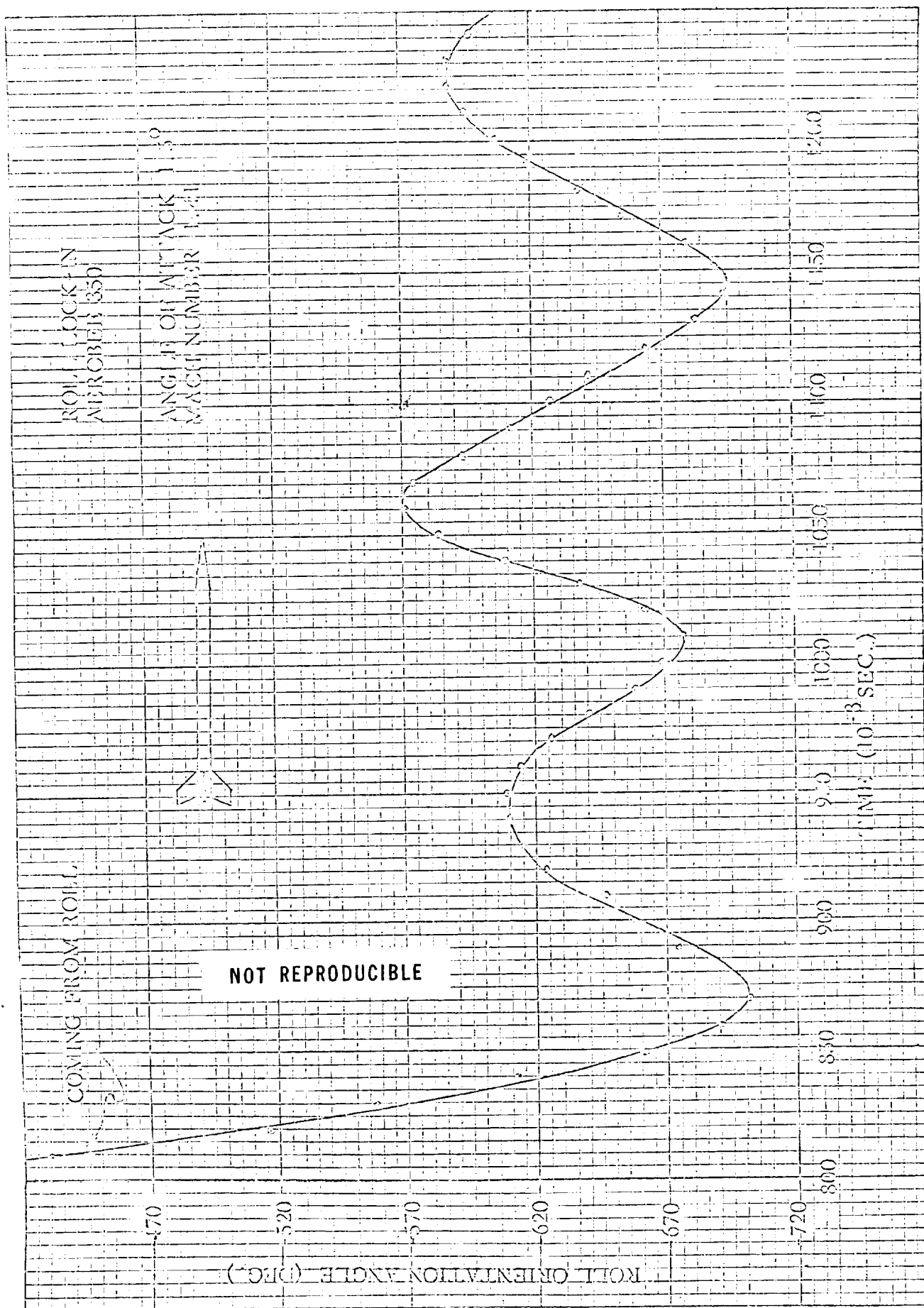


FIGURE 20c

